Occult Cardiac Contractile Dysfunction in Dystrophin-Deficient Children Revealed by Cardiac Magnetic Resonance Strain Imaging

M.W. Ashford, Jr, MD; W. Liu, PhD; S.J. Lin, MSEE; P. Abraszewski, MD; S.D. Caruthers, PhD; A.M. Connolly, MD; X. Yu, ScD; S.A. Wickline, MD

Background—Duchenne muscular dystrophy (DMD) is an inherited disease characterized by early onset of skeletal muscle degeneration and progressive weakness. Although dilated cardiomyopathy may occur during adolescence, it is often undetected early in its course because of physical inactivity and generalized debilitation. The purpose of this study was to apply the technique of cardiac magnetic resonance (CMR) tagging to detect occult cardiac dysfunction in young subjects with DMD by measuring myocardial strain and torsion.

Methods and Results—Thirteen DMD pediatric subjects without clinically apparent heart disease and 9 age-matched healthy males were recruited. Each was scanned on a 1.5-T clinical scanner to acquire contiguous short-axis planes from the apex to the mitral valve plane and then 3 tagged images at base, midventricle, and apex. Global and segmental myocardial net twist and circumferential strain were computed with the use of 2D homogeneous strain analysis. Ventricular torsion was computed by normalizing net twist by the distance from apex to mitral valve plane. DMD patients exhibited normal left ventricular volumes and ejection fractions but manifested reduced midventricular and basal cross-sectional global circumferential strain compared with the reference group ($P<0.005$). These alterations also appeared in segmental analyses in the septal, anterior, lateral, and inferior walls ($P<0.05$).

Conclusions—In patients predisposed to cardiomyopathies because of dystrophinopathy, occult regional cardiac dysfunction can be diagnosed with CMR tagging. This method of strain imaging analysis may offer a sensitive approach for delineating the presence and progression of cardiovascular disease and for assessing therapies designed to modulate the onset and course of heart failure. **(*Circulation*. 2005;112:2462-2467.)**

Key Words: cardiomyopathy ■ muscular dystrophy, Duchenne ■ heart failure ■ torsion, left ventricular ■ magnetic resonance imaging

The dystrophinopathies comprise a group of X-linked genetic diseases that feature dystrophin deficiency–Duchenne muscular dystrophy (DMD), Becker muscular dystrophy, and X-linked dilative cardiomyopathy. Each is characterized by progressive weakness and wasting of skeletal, smooth, and cardiac muscle but without primary structural abnormalities in the lower motor neuron or other neuromuscular process.[1–4] DMD is the most severe dystrophinopathy, and with an incidence of 1:3500 male births, it accounts for >80% of the dystrophinopathies.[3–5]

Cardiac manifestations include cardiomyopathy, conduction system dysfunction, eventual heart failure, and sudden death. Approximately 96% of DMD subjects will develop evidence of cardiomyopathy during adolescence.[1,4,6] Although dilated cardiomyopathy may initially occur during adolescence, it is often detected late in its course because of physical inactivity and generalized debilitation. Because the risk of mortality and morbidity secondary to pulmonary causes has declined as a result of advances in respiratory therapy, cardiomyopathy is emerging as a common cause of death in DMD patients.[1,7]

Given the manifold challenges for both early detection and quantitative assessment of cardiac deficiency in these patients, we hypothesized that cardiac magnetic resonance (CMR) imaging might offer a more sensitive, noninvasive approach for phenotypic characterization of occult functional features of DMD cardiomyopathy. "MRI tagging" approaches enable accurate and rapid measurement of regional transmural myocardial deformation over the entire cardiac cycle.[8–10] This technique involves selective manipulation of tissue magnetization to create transient deformable markers, or "tags," that uniquely depict complex intramyocardial kinetics in the contracting heart. Analysis of tag deformation to delineate abnormal tissue strain patterns could serve to

Received November 1, 2004; revision received August 1, 2005; accepted August 3, 2005.

From the Departments of Medicine (M.W.A., W.L., S.J.L., P.A., S.D.C., X.Y., S.A.W.), Neurology, and Pediatrics (A.M.C.), and Biomedical Engineering (W.L., X.Y., S.A.W.), Washington University School of Medicine, St Louis, Mo, and Philips Medical Systems, Best, Netherlands (S.D.C.).

Correspondence to Samuel A. Wickline, MD, Cardiovascular Division, Campus Box 8086, 660 S Euclid Ave, St Louis, MO 63110. E-mail saw@wuphys.wustl.edu

Circulation **is available at http://www.circulationaha.org** **DOI: 10.1161/CIRCULATIONAHA.104.516716**

TABLE 1. Physical Characteristics of DMD and Reference Subjects

	DMD (n=13)	Reference (n=9)	*P*
Age, y	10.6±3.01	11.1±2.53	0.67
Weight, kg	49.6±26.1	41.4±10.1	0.24
Height, cm	142.9±23.4	147.5±14.4	0.77
Body mass index, kg/m^2	21.1±5.79	18.9±3.81	0.37
Ambulatory	10 of 13	9 of 9	N/A
Corticosteroid use	11 of 13	0 of 9	N/A

Values are mean±SD.

quantify preclinical features of cardiac dysfunction. Such an approach might foster earlier application of clinical regimens to prevent cardiac dysfunction rather than delaying intervention until the appearance of signs such as ventricular dilatation and reduced ejection fraction that typify the later stages of DMD.

We conducted a pilot study to characterize cardiac function with the use of CMR in a cohort of young outpatients with classic musculoskeletal signs of DMD but without apparent clinical cardiac dysfunction compared with an age-matched reference cohort. Routine CMR and tagging were performed expeditiously in these unsedated boys, revealing normal global cardiac function according to traditional measures of ejection fraction and cavity anatomy. However, tagging analysis revealed marked changes in cardiac tissue kinetics that may serve as harbingers of incipient cardiac failure and suggest a strategy for earlier evaluation and treatment and closer follow-up for the purpose of preventing progressive cardiac deterioration.

Methods

Patient Recruitment

Thirteen patients confirmed to have DMD by biopsy, elevated creatine kinase, or DNA analysis but without known heart disease were recruited from the Neuromuscular Clinic at Washington University in St Louis, Mo, by one of the authors (A.M.C.) without prior knowledge of ventricular function. Nine age-matched healthy males were recruited independently by staff members of the Cardiovascular Magnetic Resonance Laboratory from a population of children who were relatives or friends of the authors without prior knowledge of their cardiac function. An attempt was made to recruit patients of approximately the same age as the DMD patients. These patients were enrolled in the study over a 20-month period. General exclusion criteria included the presence of metal parts, such as shrapnel, permanent cardiac pacemakers, metal splinters, or other general contraindications to MRI, although none of the DMD or healthy reference subjects actually were excluded for these reasons. All subjects were under the age of 18 years, and eligibility criteria (besides age and DMD) included only a willingness to undergo an MRI examination. Physical and clinical characteristics are listed in Table 1. Written informed consent was obtained from each parent before the study, which was approved by the institutional review board of the Washington University Medical Center.

DMD subjects unable to walk without assistance underwent pulmonary function testing as part of their management. Musculoskeletal strength in both upper and lower extremities was routinely measured during clinic visits. Medication history, particularly corticosteroid use, was reviewed for each patient.

Magnetic Resonance Imaging

MRI experiments were conducted on a 1.5-T Intera whole-body MR system (Philips Medical Systems). Cine images of contiguous nonoverlapping short-axis planes from the mitral valve plane to the apex were obtained with the use of an ECG-triggered gradient-echo sequence. Acquisition variables were as follows: repetition time, 3.3 ms; echo time, 1.65 ms; flip angle, 50 degrees; field of view, 400 mm; acquisition matrix, 256×256; and slice thickness, 12 mm.

To describe the regional and global motion of the myocardium, a set of 3 tagged images was acquired. Apical, midventricular, and basal short-axis slices were tagged by applying 2 orthogonal spatial modulations of magnetization (SPAMM) pulses at end-diastole, which yielded tag grid spacing of 6 mm. Tag displacement was tracked throughout the cardiac cycle by acquiring gradient echo cine images. Imaging variables included the following: repetition time, 25 ms; echo time, 5 ms; flip angle, 13 degrees; field of view, 330 mm; acquisition matrix, 256×256; and slice thickness, 8 mm. Tagging throughout the entire cardiac cycle required 20 frames.

Data Analysis

Images were analyzed with the use of a MATLAB-based computer program developed in our laboratory that quantified 2D regional wall motion within the myocardium.[11] Epicardial and endocardial borders were manually and interactively traced throughout the entire cardiac cycle (starting at end-diastole) in each temporal frame of the cine images with the B-spline method.[12] The left ventricle was divided into 4 regions: anterior, lateral, inferior, and septum. Segmental ventricular wall thickness also was calculated.

To determine regional myocardial wall motion, tagging lines and intersection tagging points were semiautomatically traced throughout the cardiac cycle. The myocardium was then partitioned into nonoverlapping triangular elements with sets of adjacent tag points used as vertices.[13] The deformation of each triangle defined regional wall motion across the ventricular short-axis plane by using finite element methods to quantify left ventricular twist, circumferential shortening, and circumferential strain.

Twist was defined as the rotation angle of the centroid of the triangular element about the left ventricular cavity center; positive angle indicated clockwise twist as viewed from the base. Under the assumption that the myocardium was homogeneous locally, the 2D Lagrangian strain tensor was calculated for each triangular element. The strain tensor was subsequently transformed to a local coordinate system to yield the circumferential strain. By convention, negative circumferential strain denoted shortening in the circumferential direction. Ventricular torsion was obtained by normalizing overall twist (apex minus base) by the distance from apex to mitral valve plane.

Left and right ventricular ejection fractions for all subjects were calculated by tracing the end-diastolic and end-systolic endocardial contours from CMR functional scans with the cardiac analysis package on the Philips EasyVision workstation. The analysis follows the standard methods previously reported from our laboratory and others.[14,15] For left ventricular mass, epicardial and endocardial contours for each contiguous slice were used to calculate myocardial volume (determined at end-diastole from Simpson's rule) and then multiplied by myocardial density (≈1.05 g/cm^3) to obtain mass.

Statistical Analysis

All statistical analyses were performed with the use of the procedures of the SAS Institute. Unpaired Student *t* test was used to assess differences in the means between groups where appropriate. The effects of the cardiac contractile dysfunction were tested by repeated-measures ANOVA to account for potential within-subject correlations of circumferential strain across apical, midventricular, and basal cross sections (global and regional: anterior, septal, inferior, and lateral). Receiver operator characteristic (ROC) analysis was performed to define suitable values for the detection of abnormal ventricular strain. Mean and SD for the variables of interest were determined for both groups, and probability values ≤0.05 were considered significant.

TABLE 2. Cardiovascular Characteristics of DMD and Reference Subjects

	DMD	Reference	*P*
Heart rate, bpm	94±6.4	77.8±7.6	<0.01
LV end-systolic volume, mL/m²*	13.3±4.1	15.9±4.0	0.22
LV end-diastolic volume, mL/m²*	40.1±4.1	41.8±7.8	0.57
LVEF, %/m²*	31.8±6.0	31.6±11.5	0.96
RV end-systolic volume, mL/m²*	12.2±2.6	15.1±3.9	0.08
RV end-diastolic volume, mL/m²*	32.8±5.9	33.6±6.6	0.81
RVEF, %/m²*	32.6±7.3	27.2±10.3	0.24
LV mass, g/m²*	33.6±2.9	32.4±5.5	0.55

Values are mean±SD. LV indicates left ventricular; EF, ejection fraction; and RV, right ventricular.

*Data are normalized by body surface area.

Results

Subject Characteristics

No significant differences in age or physical characteristics were noted between the DMD and reference groups (Table 1). Only 3 of 13 DMD subjects were unable to walk without assistance. Pulmonary function tests were conducted in these 3 patients, and they exhibited mild respiratory impairment according to reduced forced expiratory volume in 1 second (FEV_1) values. Each DMD subject had sufficient skeletal muscle strength to perform upper and lower body exercises during the course of strength testing. All but 2 DMD subjects were on oral corticosteroid therapy at the time of testing (on the basis of conventional practice procedures) to retard musculoskeletal deterioration.

Routine Indices of Global and Regional Cardiac Function

As displayed in Table 2, the resting heart rate of DMD subjects exceeded those of the age-matched reference patients by almost 20% (94 versus 78 bpm; $P<0.005$). However, heart rate was not found to be a significant covariant for the strain values by the general linear modeling test for slopes $\neq 0$ ($P=0.61$). Systolic blood pressures between the groups were similar (109±14 versus 102±9 mm Hg for DMD versus reference; $P=0.16$), representing equal systolic loading conditions for the ventricle, whereas the diastolic pressures were mildly higher but still normotensive for the DMD patients (66±11 versus 52±7 mm Hg for DMD versus reference; $P<0.003$). Left ventricular end-systolic and end-diastolic volumes, left ventricular mass, and left ventricular ejection fraction (all normalized by body surface area) were similar for both groups (P=NS), as were right ventricular end-systolic and end-diastolic volumes and right ventricular ejection fraction (P=NS). Wall thickness and regional thickening (normalized by body height, weight, or body mass index) also did not differ among the 2 groups (P=NS; data not shown), indicating that functional abnormalities were not apparent in typical clinical indices of left ventricular cardiac performance. Left ventricular eccentricity, the ratio of left ventricular diameter lengths, was also equivalent (≈0.8), indicating that ventricular morphology was similar.

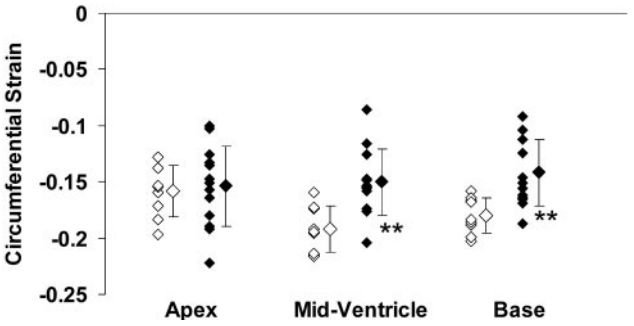

Figure 1. Segmental peak circumferential strain. The DMD group is denoted by dark diamonds. Error bars indicate±1 SD. **$P<0.005$.

MRI Tagging–Based Indices of Ventricular Function: Myocardial Strain

Figure 1 illustrates that DMD patients manifest reduced peak segmental (ie, apex-midventricle-base) circumferential strain in midventricular and basal ventricular cross sections compared with the reference group ($P<0.005$). These alterations also were apparent in global and regional (septal-anterior-lateral-inferior) data, as illustrated in Figure 2. The group differences in global circumferential strain (ie, for average circumferential strain of DMD versus reference patients) were highly significant ($F=9.15$; $P=0.0067$) by repeated-measures ANOVA. A trend toward heterogeneity of regional circumferential strain values (anterior, septal, inferior, and lateral) was manifest within the hearts of individual patients, although it did not quite attain significance ($F=3.05$; $P=0.0696$). For individual regions across the patient groups, the septal, anterior, and lateral segments differed statistically ($P=0.015$, 0.0246, 0.0052 for septal, anterior, and lateral segments, respectively), whereas the inferior wall indicated a trend toward heterogeneity ($P=0.0992$).

Myocardial Torsion

No significant differences in peak myocardial torsion were observed between the 2 groups (Figure 3).

Stratification of DMD Subjects

Disease progression and medication regimen were initially hypothesized as potential determinants of abnormal cardiovascular function and/or myocardial deformation characteristics. Clinical cardiac dysfunction or altered myocardial deformation

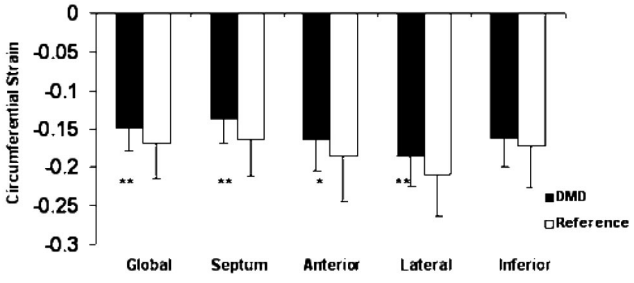

Figure 2. Global and regional peak circumferential strain. Statistical analysis by repeated-measures ANOVA. Error bars indicate ±1 SD. *$P<0.05$; **$P<0.01$.

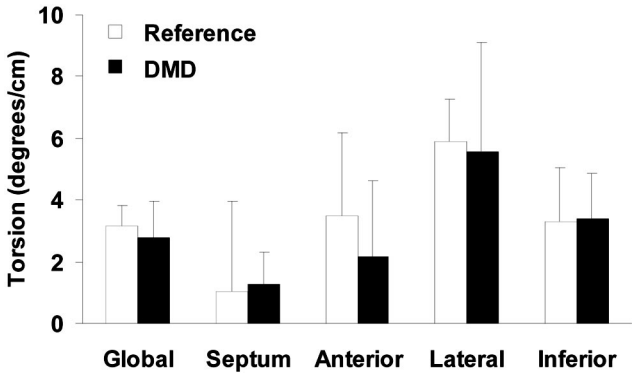

Figure 3. Global and regional peak myocardial torsion. The DMD group is denoted by dark bars. Error bars indicate±1 SD.

was not associated with corticosteroid use, ambulatory status, or musculoskeletal strength in DMD subjects.

Sensitivity and Specificity

ROC analysis of the relevant midventricular and basal circumferential strain data (Figure 4) indicates an area under the curve of ≈0.89. A circumferential strain value of −0.165 for the combined midwall and basal data results in sensitivity of 81% and specificity of 89%.

Discussion

Dystrophin is a cell membrane–associated protein located within the sarcolemma of both cardiac and skeletal muscle cells and serves multiple functions important to the maintenance of structural integrity and cardiac dynamic function. It provides structural support to the cells.[5,16,17] As a component of the dystrophin-glycoprotein complex within the sarcolemma, dystrophin serves an important role in the transduction of physical forces in striated muscle.[17] Dystrophin also contributes to signaling within cardiac and skeletal muscle cells as its presence within the dystrophin-glycoprotein complex enables molecules such as neuronal nitric oxide synthase and voltage-gated sodium channels to attach onto this complex. Dystrophin is known to interact with calmodulin, a regulator of calcium-dependent kinases and hence contractility. Additionally, dystrophin is involved with regulating intramuscular blood flow, which has been shown in the *mdx* mouse to be associated with either the production or transmission of an intracellular signal from muscle fibers to the vascular endothelium.[18]

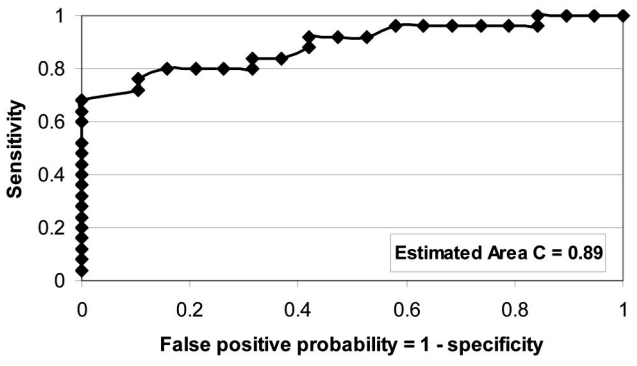

Figure 4. ROC analysis for circumferential midventricular and base strain data values for each patient.

Given these critical roles, it is not surprising that >20% of patients with DMD die of cardiac disease, generally during early adulthood.[4,19] The present data represent the first demonstration of a sensitive and specific method to quantify the incipient deleterious effects of this disease on cardiac function at the tissue level, well in advance of the emergence of overt cardiovascular signs and symptoms. DMD patients frequently present with clinical cardiac symptoms at age >15 years, with the majority reporting cardiovascular symptoms when they are aged >18 years.[4] In this report, the use of CMR tagging allowed delineation of occult cardiac involvement in a cohort whose average age was only 11 years. Despite the presumed challenges of imaging these affected individuals, we observed that most of these patients and their families are highly motivated and that cardiac imaging could be accomplished with excellent patient cooperation and satisfaction.

The DMD subjects exhibited decreased global, segmental, and regional circumferential strain (Figures 1 and 2). Three of 4 regions manifested significantly decreased circumferential strain, as did the basal and midventricular segments by repeated-measures ANOVA. In contrast to the present findings, previous investigations with standard echocardiography and radionuclide imaging have reported the primary defects of cardiac involvement in DMD to reside within the inferior[20,21] or posterolateral walls.[22] The reason for this difference most probably reflects the enhanced sensitivity of CMR for detecting widespread but subtle changes of intramural contractile function, which are interpretable only at regional or global levels with the use of alternative technologies.

It is possible that Doppler tissue velocity imaging and strain rate imaging could offer additional sensitivity for such diagnosis at the tissue level in the future.[23] Indeed, a recent report from Chetboul et al[24] indicates that preclinical detection of reduced strain rate, or myocardial tissue velocity, in the posterior wall of Golden Retriever dogs, a congenital dystrophinopathy and a model for DMD, is possible with tissue Doppler imaging of segments accessible to ultrasound. In these cases, the left ventricular ejection fraction and fractional wall shortening values also were not statistically different despite the reduced segmental velocities. Although the tissue Doppler data are not strictly comparable to the MRI tagging information because they report strain rate rather than absolute strain magnitude, the 2 studies are consistent in their detection of the early manifestations of abnormal strain indexes that precede any detectable changes in wall thickening or ejection fraction. Because MRI is known to be the more reproducible method for defining left ventricular ejection fraction in humans, we have used the most robust measure available for comparison with the intramural strain data.[15]

Certain features of myocardial function, such as torsion, are well preserved, whereas others, specifically circumferential strain, exhibit early abnormalities that may presage eventual heart failure. It is possible that the ability of the heart to maintain ventricular torsion results in preserved global ventricular function for some time, despite the concurrent

appearance of early cardiac dysfunction. We did not measure 3D strain indexes by tagging and therefore cannot comment on alternative fundamental mechanisms of contractile compensation that might preserve torsion and global ventricular function in the face of mild decrements in other fiber strain values. As the disease progresses, myocytes are replaced with increasing amounts of connective tissue as the adaptive repair of dystrophic sarcomeres becomes less efficient.[16] The gradual loss of sarcomeres results in unfavorable changes in myocardial contractility, as manifested by decreased circumferential strain early, decreased torsion later, and eventually decreased ejection fraction and clinical heart failure.

Cardiomyopathy Detection and Surveillance

Most of these patients were undergoing therapy with corticosteroids in an attempt to preserve skeletal and respiratory muscle strength. It is also possible that preservation of left ventricular function was achieved by steroid therapy, which could form the basis for additional hypothesis testing with the use of the quantitative CMR tagging methods to follow therapy aimed at maintaining cardiac function. Although stratification did not reveal differences in DMD subjects on versus off steroids in terms of cardiac function, our study was not designed a priori or appropriately powered post hoc to elucidate these effects. Nevertheless, Ishikawa et al[1] and Ramaciotti et al[25] investigated the relationship of neurohormonal activity to the extent of cardiomyopathy in DMD patients with the former demonstrating that angiotensin-converting enzyme inhibitors and β-blockers can reverse signs and symptoms of congestive heart failure in this group. Mori et al[26] found that the technique of integrated ultrasound backscatter (IBS) could detect early evidence of cardiomyopathy in DMD patients as both the magnitudes of cyclic variation and IBS intensity are reduced in DMD patients. Suwa et al[27] reported that myocardial IBS intensity could be used to predict the degree of myocardial fibrosis and the response to β-blocker therapy in DMD patients. Recent data from Vatta and associates[17,28] further illustrate the potential for reversing the loss of cardiac dysfunction that accompanies other forms of heart failure with the use of afterload-reducing ventricular assist devices.

Study Limitations

Although significant differences were observed in circumferential strain when DMD subjects were compared with age-matched reference patients in this study, these findings were subtle. Caution should be exercised in applying these particular criteria to the diagnosis of DMD cardiomyopathy in the general population, however, since the current group of patients was being treated with steroid therapy, which might attenuate the differences in strain. In addition, in view of the modest sample sizes in this pilot study, we may have been statistically underpowered to detect moderate differences between true means of populations from which these samples were drawn. Accordingly, an examination of a larger group of untreated patients would be required to provide generally predictive strain values.

The blood pressure measurements in the DMD versus reference patients revealed no differences in systolic afterloading conditions, but diastolic pressures were slightly higher but within normal limits, perhaps as a result of the steroid use. Although reduced "circumferential shortening" has been reported for frankly hypertrophic ventricles in patients with systolic/diastolic hypertensive hypertrophy,[29] the left ventricular mass was normal in these DMD cases, as was the afterload. Thus, the potential impact of pure preload alterations on systolic mechanics and active tissue strain in DMD patients without left ventricular hypertrophy is difficult to assess but should be kept in mind.

The average age of these DMD subjects was 11 years, whereas DMD subjects reportedly do not exhibit clinical cardiovascular compromise until approximately the age of 15 years by other criteria.[19] Regional wall motion abnormalities, ventricular dilatation, and decreased left ventricular function have been reported in older patients with the use of echocardiography.[20,30,31] Future studies of myocardial strain and torsion in both older and younger populations should help to elucidate the range and heterogeneity of cardiac dysfunction and its exact age dependency. Regardless, the data illustrate the sensitivity of the method for defining early changes throughout the heart that might serve as predictors of eventual heart failure, and as such they would represent important and unique markers applicable for early diagnosis and longitudinal evaluation in individual patients.

Clinical Implications

Because half of DMD carriers have evidence of heart disease leading to death or heart transplantation,[4,32,33] CMR tagging could be utilized to detect early cardiac involvement as well as to monitor and quantify the effects of novel therapeutic approaches. For example, therapies such as growth hormone administration in humans[34] or gene therapies to replace dystrophin[35] and utrophin[36] in animal models can be assessed at the cardiac tissue level. We propose that widespread adoption of these methods in future multicenter clinical trials could facilitate discovery of improved treatment strategies for reducing cardiovascular morbidity and mortality in DMD, much as longevity has been extended in the adult population suffering heart failure from other diverse etiologies.

Acknowledgments

This study was supported by grants from the American Heart Association (0215174Z and 0325469Z), the National Institutes of Health (HL-42950 and HL-73315), Philips Medical Systems, and the Edith and Alan Wolfe Charitable Trust. We wish to recognize the important contributions of Peggy Brown, Junjie Chen, Lynn Coulter, Katherine A. Lehr, Mary P. Watkins, and Todd A. Williams to this project, specifically involving patient recruitment and imaging.

Disclosure

Dr Caruthers is an employee of Philips Medical Systems; has served as an unpaid consultant on multiple grants from the NIH; and owns stock in Koninklijke Philips Electronics. Dr Liu is an employee of Philips Medical Systems. Philips Medical Systems makes and sells the MRI scanners used in this study.

References

1. Ishikawa Y, Bach JR, Minami R. Cardioprotection for Duchenne's muscular dystrophy. *Am Heart J*. 1999;137:895–902.
2. Roland EH. Muscular dystrophy. *Pediatr Rev*. 2000;21:233–237.
3. Emery AE. Muscular dystrophy into the new millennium. *Neuromuscul Disord*. 2002;12:343–349.

4. Finsterer J, Stollberger C. The heart in human dystrophinopathies. *Cardiology*. 2003;99:1–19.
5. Biggar WD, Klamut HJ, Demacio PC, Stevens DJ, Ray PN Duchenne muscular dystrophy: current knowledge, treatment, and future prospects. *Clin Orthop*. 2002;88–106.
6. Yue Y, Li Z, Harper SQ, Davisson RL, Chamberlain JS, Duan D. Microdystrophin gene therapy of cardiomyopathy restores dystrophin-glycoprotein complex and improves sarcolemma integrity in the *mdx* mouse heart. *Circulation*. 2003;108:1626–1632.
7. Bach JR. Update and perspective on noninvasive respiratory muscle aids, part 2: the expiratory aids. *Chest*. 1994;105:1538–1544.
8. Axel L, Dougherty L. Heart wall motion: improved method of spatial modulation of magnetization for MR imaging. *Radiology*. 1989;172: 349–350.
9. Moore CC, McVeigh ER, Zerhouni EA. Quantitative tagged magnetic resonance imaging of the normal human left ventricle. *Top Magn Reson Imaging*. 2000;11:359–371.
10. Sandstede JJ, Johnson T, Harre K, Beer M, Hofmann S, Pabst T, Kenn W, Voelker W, Neubauer S, Hahn D. Cardiac systolic rotation and contraction before and after valve replacement for aortic stenosis: a myocardial tagging study using MR imaging. *AJR Am J Roentgenol*. 2002; 178:953–958.
11. Liu W, Chen J, Ji S, Allen JS, Bayly PV, Wickline SA, Yu X. Harmonic phase MR tagging for direct quantification of Lagrangian strain in rat hearts after myocardial infarction. *Magn Reson Med*. 2004;52: 1282–1290.
12. Radeva P, Amini AA, Huang J. Deformable B-solids and implicit snakes for 3D localization and tracking of SPAMM MRI data. *Comput Vis Image Und*. 1997;66:163–178.
13. Chandrupatla TR, Belegundu A. *Introduction to Finite Elements in Engineering*. Englewood Cliffs, NJ: Prentice Hall; 1996.
14. Lorenz CH, Walker ES, Morgan VL, Klein SS, Graham TP Jr. Normal human right and left ventricular mass, systolic function, and gender differences by cine magnetic resonance imaging. *J Cardiovasc Magn Reson*. 1999;1:7–21.
15. Pennell DJ. Ventricular volume and mass by CMR. *J Cardiovasc Magn Reson*. 2002;4:507–513.
16. Grady RM, Teng H, Nichol MC, Cunningham JC, Wilkinson RS, Sanes JR. Skeletal and cardiac myopathies in mice lacking utrophin and dystrophin: a model for Duchenne muscular dystrophy. *Cell*. 1997;90: 729–738.
17. Vatta M, Stetson SJ, Perez-Verdia A, Entman ML, Noon GP, Torre-Amione G, Bowles NE, Towbin JA. Molecular remodelling of dystrophin in patients with end-stage cardiomyopathies and reversal in patients on assistance-device therapy. *Lancet*. 2002;359:936–941.
18. Grady RM, Grange RW, Lau KS, Maimone MM, Nichol MC, Stull JT, Sanes JR. Role for alpha-dystrobrevin in the pathogenesis of dystrophin-dependent muscular dystrophies. *Nat Cell Biol*. 1999;1:215–220.
19. Metules T. Duchenne muscular dystrophy. *RN*. 2002;65:39–44.
20. de Kermadec JM, Becane HM, Chenard A, Tertrain F, Weiss Y, Davis RC. Prevalence of left ventricular systolic dysfunction in Duchenne muscular dystrophy: an echocardiographic study. *Am Heart J*. 1994;127: 618–623.
21. Perloff JK, Henze E, Schelbert HR. Alterations in regional myocardial metabolism, perfusion, and wall motion in Duchenne muscular dystrophy studied by radionuclide imaging. *Circulation*. 1984;69:33–42.
22. Emery AE. Some unanswered questions in Duchenne muscular dystrophy. *Neuromuscul Disord*. 1994;4:301–303.
23. Abraham TP, Nishimura RA, Holmes DR Jr, Belohlavek M, Seward JB. Strain rate imaging for assessment of regional myocardial function: results from a clinical model of septal ablation. *Circulation*. 2002;105: 1403–1406.
24. Chetboul V, Escriou C, Tessier D, Richard V, Pouchelon J, Thibault H, Lallemand F, Thuillez C, Blot S, Derumeaux G. Tissue Doppler imaging detects early asymptomatic myocardial abnormalities in a dog model of Duchenne's cardiomyopathy. *Eur Heart J*. 2004;25:1934–1939.
25. Ramaciotti C, Scott WA, Lemler MS, Haverland C, Iannaccone ST. Assessment of cardiac function in adolescents with Duchenne muscular dystrophy: importance of neurohormones. *J Child Neurol*. 2002;17: 191–194.
26. Mori K, Manabe T, Nii M, Hayabuchi Y, Kuroda Y, Tatara K. Myocardial integrated ultrasound backscatter in patients with Duchenne's progressive muscular dystrophy. *Heart*. 2001;86:341–342.
27. Suwa M, Ito T, Kobashi A, Yagi H, Terasaki F, Hirota Y, Kawamura K. Myocardial integrated ultrasonic backscatter in patients with dilated cardiomyopathy: prediction of response to beta-blocker therapy. *Am Heart J*. 2000;139:905–912.
28. Vatta M, Stetson SJ, Jimenez S, Entman ML, Noon GP, Bowles NE, Towbin JA, Torre-Amione G. Molecular normalization of dystrophin in the failing left and right ventricle of patients treated with either pulsatile or continuous flow-type ventricular assist devices. *J Am Coll Cardiol*. 2004;43:811–817.
29. Palmon LC, Reichek N, Yeon SB, Clark NR, Brownson D, Hoffman E, Axel L. Intramural myocardial shortening in hypertensive left ventricular hypertrophy with normal pump function. *Circulation*. 1994;89:122–131.
30. Heymsfield SB, McNish T, Perkins JV, Felner JM. Sequence of cardiac changes in Duchenne muscular dystrophy. *Am Heart J*. 1978;95:283–294.
31. Goldberg SJ, Stern LZ, Feldman L, Allen HD, Sahn DJ, Valdes-Cruz LM. Serial two-dimensional echocardiography in Duchenne muscular dystrophy. *Neurology*. 1982;32:1101–1105.
32. Kamakura K, Kawai M, Arahata K, Koizumi H, Watanabe K, Sugita H. A manifesting carrier of Duchenne muscular dystrophy with severe myocardial symptoms. *J Neurol*. 1990;237:483–485.
33. Hoogerwaard EM, van der Wouw PA, Wilde AA, Bakker E, Ippel PF, Oosterwijk JC, Majoor-Krakauer DF, van Essen AJ, Leschot NJ, de Visser M. Cardiac involvement in carriers of Duchenne and Becker muscular dystrophy. *Neuromuscul Disord*. 1999;9:347–351.
34. Cittadini A, Ines Comi L, Longobardi S, Rocco Petretta V, Casaburi C, Passamano L, Merola B, Durante-Mangoni E, Sacca L, Politano L. A preliminary randomized study of growth hormone administration in Becker and Duchenne muscular dystrophies. *Eur Heart J*. 2003;24: 664–672.
35. Clemens PR, Kochanek S, Sunada Y, Chan S, Chen HH, Campbell KP, Caskey CT. In vivo muscle gene transfer of full-length dystrophin with an adenoviral vector that lacks all viral genes. *Gene Ther*. 1996;3:965–972.
36. Cerletti M, Negri T, Cozzi F, Colpo R, Andreetta F, Croci D, Davies KE, Cornelio F, Pozza O, Karpati G, Gilbert R, Mora M. Dystrophic phenotype of canine X-linked muscular dystrophy is mitigated by adenovirus-mediated utrophin gene transfer. *Gene Ther*. 2003;10:750–757.